Effect of Dense-to-Loose Layer Ratio in Silk Fibroin Membranes on Guided Bone Regeneration

Huilu Zhan, Linling Yin, Yiping Wang, Jinsong Pan*
Department of Stomatology, Shanghai General Hospital, Shanghai Jiao Tong University School of Medicine, Shanghai 200080, China

Abstract: Objective: To investigate the functions of silk fibroin (SF) membranes with different ratios of dense layer to loose layer in preventing fibroblast infiltration and promoting bone marrow mesenchymal stem cell (BMSC) penetration, so as to provide experimental evidence and guidance for the design of clinical guided bone regeneration membranes. Methods: SF membranes with dense-to-loose layer ratios of 1:0, 1:1, 1:2, 1:4 and 0:1 were prepared. Scanning electron microscopy (SEM) and Fourier transform infrared spectroscopy were used to characterize the material properties. Fluorescence staining was applied to detect the barrier effect of the membranes on fibroblasts and the guidance effect on BMSCs. A rat skull defect model with membrane implantation was established, and bone volume fraction was measured to evaluate the bone regeneration efficacy. Results: SEM revealed that the membrane exhibited an asymmetric structure with one dense side and one porous side. The penetration depths of fibroblasts in the 1:0, 1:1, 1:2 and 1:4 groups were significantly lower than those in the 0:1 group. The penetration depths of BMSCs in the 1:2, 1:4 and 0:1 groups were significantly higher than those in the 1:0 group. The rat skull defect experiment showed that the bone volume fractions in the 1:2 and 1:4 groups were higher than those in other groups. Conclusion: When the ratio of dense-to-loose layer of SF membrane is designed between 1:2 and 1:4, it can simultaneously achieve favorable barrier function and stem cell guidance ability, thereby effectively promoting bone regeneration.
***Keywords*:** silk fibroin, guided bone regeneration, bone defect

1. Introduction

Guided bone regeneration (GBR) is a core clinical technique for the treatment of alveolar bone defects, which is widely used in oral diseases such as periodontal diseases and peri-implant bone defects. Its core principle is to construct a physical barrier via membrane to block the abnormal invasion of soft tissues and fibroblasts into the bone defect area, while providing a suitable microenvironment for the adhesion, proliferation and differentiation of osteogenic cells, and ultimately achieving the repair and regeneration of bone defects [1-3]. However, traditional GBR membranes commonly used in clinical practice still have many limitations. For example, non-resorbable membranes (such as polytetrafluoroethylene membranes) have certain physical barrier functions but poor biocompatibility and non-degradability, requiring secondary surgical removal and increasing patient suffering [4]. Resorbable membranes (such as collagen membranes) have favorable biocompatibility, but insufficient physical strength, weak barrier function, easily collapse, and limited osteogenic induction activity [5-7]. Therefore, developing a novel GBR membrane with excellent physical barrier function, osteogenic induction activity and biocompatibility has become a research hotspot in the field of oral biomaterials.

As a natural biological macromolecule material, silk fibroin has excellent biocompatibility, degradability and favorable mechanical properties. Its degradation products are non-toxic and harmless, which can be metabolized and absorbed by the body, and have been widely used in tissue engineering, drug delivery and other fields [8-9]. The SF membrane in this study is designed based on an asymmetric structure of "one dense side and one porous side", breaking the limitation of the "single structure" of traditional membranes. The dense side can build a solid physical barrier to effectively block the excessive proliferation and invasion of fibroblasts into the bone defect area, avoiding the interference of soft tissue ingrowth on bone regeneration. The porous side can simulate the biomimetic microenvironment of natural bone tissue, providing a stable channel for the adhesion, proliferation and penetration of bone marrow mesenchymal stem cells (BMSCs), promoting the migration and differentiation of osteogenic cells, and thus accelerating bone tissue regeneration [10-11].

The structural characteristics of GBR membranes are closely related to their functions, and the ratio of dense layer to loose layer, as a core design parameter, directly affects the barrier performance and osteogenic induction ability of membrane. At present, the research on the effects of different layer ratios of SF membranes on related cell behaviors is not clear, and reasonable layer ratio design still lacks experimental evidence. In this study, by preparing SF membranes with different dense-to-loose layer ratios, we systematically explored their barrier effect on fibroblast infiltration and guidance effect on BMSC penetration, verified their in vivo bone regeneration efficacy through animal experiments, clarified the optimal

membrane layer ratio range, and provided theoretical support and experimental guidance for the design and application of novel clinical GBR membrane.

2. Materials and methods

2.1 Preparation of SF membranes with different ratios

SF membranes with different dense-to-loose layer ratios were prepared by the particle leaching method. The specific steps were as follows: A 10% (mass concentration) SF solution was prepared. Different masses of sodium chloride particles with a particle size of 75–150 μm were weighed and evenly spread on the bottom of the mold. The same volume of SF solution was added, and the mixture was frozen in a −80 °C refrigerator for 24 h, then freeze-dried in a freeze dryer for 48 h. After ethanol crosslinking and pure water washing, SF membranes were obtained. Membranes with dense-to-loose layer ratios of 1:0 (SF1:0, dense layer only), 1:1 (SF1:1), 1:2 (SF1:2), 1:4 (SF1:4) and 0:1 (SF0:1, loose layer only) were prepared respectively. After sterilization with 75% ethanol, the membranes were stored in a sterile environment for later use.

2.2 SEM characterization

The dried SF membranes were pasted on the sample stage with conductive adhesive with the smooth side or rough side upward. To observe the cross-sectional morphology, the membranes were quickly frozen in liquid nitrogen and then snapped off immediately. Care was taken to avoid contact with the cross-section during operation to prevent structural damage. Then the cross-sectional samples were vertically pasted on the side of the observation stage with conductive adhesive, so that the cross-section was slightly higher than the stage surface. The samples were sputter-coated with gold under low vacuum conditions, and the surface structure was observed by SEM at an accelerating voltage of 5 kV.

2.3 FTIR analysis

The chemical structures of SF membranes with different ratios were detected by FTIR spectrometer. The scanning range was 400–4000 cm^{-1} with a resolution of 4 cm^{-1} to analyze the characteristic absorption peaks of the membranes.

2.4 Detection of fibroblast barrier function

SF membranes with different ratios were spread on the bottom of 24-well plates, respectively. After digestion, fibroblast cell suspension and 600 μL of DMEM high-glucose medium containing 10% fetal bovine serum were added, and cultured in a 37 °C, 5% CO_2 incubator for 5 days. After culture, the SF membranes were taken out, washed 3 times with PBS, fixed with 4% paraformaldehyde for 30 min, stained with DAPI staining solution for 10 min, observed and photographed under a fluorescence microscope. The penetration depth of fibroblasts into the membrane was measured, and 4 visual fields were randomly selected for each group to calculate the average value.

2.5 Detection of BMSC guidance function

BMSC suspension was added using the same method as 2.4, and cultured with 600 μL of DMEM medium containing 10% fetal bovine serum for 5 days. After culture, the membranes were washed 3 times with PBS, stained with live cell staining solution at 37 °C for 15 min, observed and photographed under a fluorescence microscope. The penetration depth of BMSCs into the membrane was measured, and 4 visual fields were randomly selected for each group to calculate the average value.

2.6 Establishment and treatment of rat skull defect model

Thirty-six SPF-grade SD rats were randomly divided into 6 groups (n=6): blank group (no material implanted), SF1:0, SF1:1, SF1:2, SF1:4 and SF0:1 group. Rats were anesthetized by intraperitoneal injection of Zoletil 50 (25 mg/kg). After depilation and disinfection of the head, a longitudinal incision was made along the midline of the skull, the scalp and periosteum were separated to expose the skull. A circular defect with a diameter of 5 mm was prepared on the right side of the skull using a trephine (depth to the inner plate of the skull without damaging the dura mater). The blank group only received defect preparation without any material implantation; in the other groups, SF membranes with corresponding ratios were cut into discs with a diameter of 6 mm and implanted into the defect area to ensure close fit between the membrane and the bone defect. The scalp was sutured, and penicillin (100,000 U per rat) was injected intramuscularly for 3 consecutive days after surgery to prevent infection. The rats were fed routinely with free access to food and water. After 8 weeks of feeding, the rats were euthanized, and the harvested rat skull tissues were scanned in a micro-CT scanner. Caliper Analyze software was used for reconstruction and analysis of the scanned images, and the bone volume fraction (BV/TV) of the bone defect area in each group was measured, i.e., the ratio of bone tissue volume to total volume of the defect area. This study was approved by the Animal Ethics Committee of Shanghai Ninth People's Hospital, Shanghai Jiao Tong University School of Medicine (approval number: SH9H-2026-A1-1).

2.7 Statistical analysis

SPSS 22.0 statistical software was used for data analysis. Measurement data were expressed as mean ± standard deviation ($\bar{x}\pm s$). One-way analysis of variance (One-Way ANOVA) was used for comparison between groups. After homogeneity test of variance, LSD test was used for pairwise comparison. Welch test and Brown-Forsythe test were used for correction when variance was heterogeneous. $P<0.05$ was considered statistically significant.

3. Results

3.1 SEM morphology observation of membranes in each group

The SF1:0 group only showed a dense layer structure with a smooth surface, no obvious pores and no loose porous area. The SF1:1 group showed a typical asymmetric structure of "half dense and half porous". The dense side had a smooth and compact surface, and the porous side had uniform pore distribution with a pore size of 75–150 μm and good pore connectivity. The proportion of loose layer in SF1:1, SF1:2 and SF1:4 groups increased successively. The SF0:1 group only showed a loose layer structure with pores covering the entire surface. The results showed that the SF membranes prepared in this study successfully achieved the asymmetric structure design, and the microstructures of membranes with different ratios were significantly different (Figure 1).

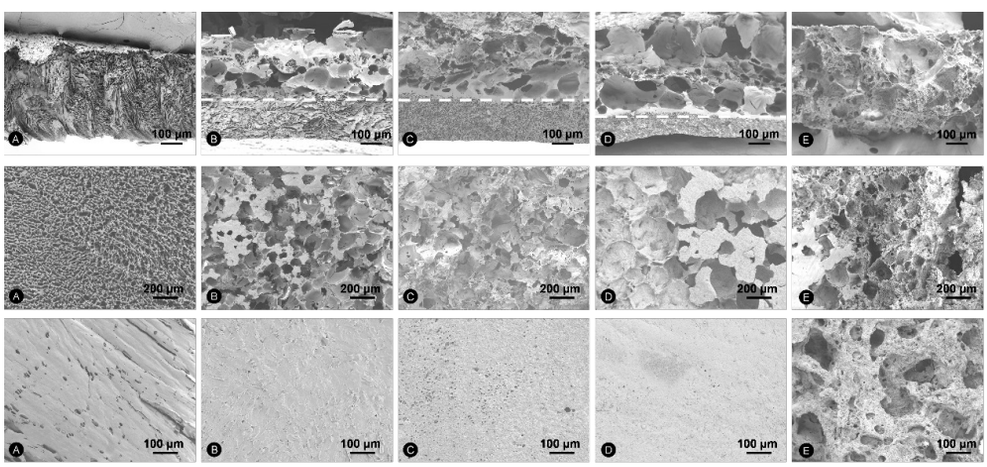

Figure 1. SEM images of SF membranes with different ratios. Group A: SF1:0; Group B: SF1:1; Group C: SF1:2; Group D: SF1:4; Group E: SF0:1.

3.2 FTIR analysis

FTIR results showed that SF membranes with different ratios all displayed typical characteristic absorption peaks of silk fibroin at 1650 cm^{-1} (Amide I band, C=O stretching vibration), 1540 cm^{-1} (Amide II band, N-H bending vibration) and 1240 cm^{-1} (Amide III band, C-N stretching vibration), indicating that the prepared membrane maintained the natural chemical structure of silk fibroin without obvious structural changes (Figure 2).

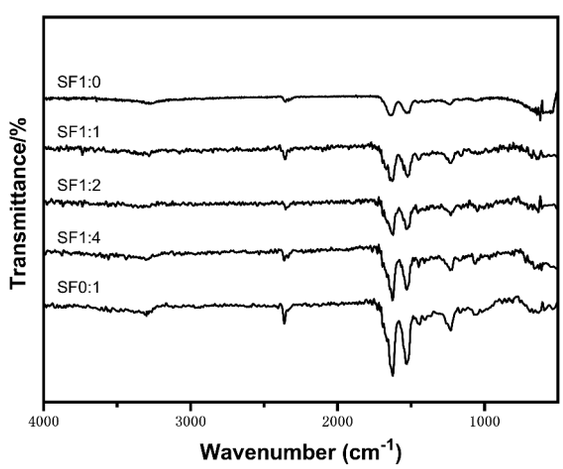

Figure 2. FTIR spectra of SF membranes in each group

3.3 Barrier function against fibroblasts

DAPI staining results of L929 fibroblasts showed varying degrees of cell penetration in each group. Compared with the SF0:1 group, the penetration depths in the other groups were significantly decreased, with statistically significant differences. There were no statistically significant differences among SF1:1, SF1:2 and SF1:4 groups, indicating that the asymmetric structure of SF membranes could effectively block fibroblast infiltration (Figure 3).

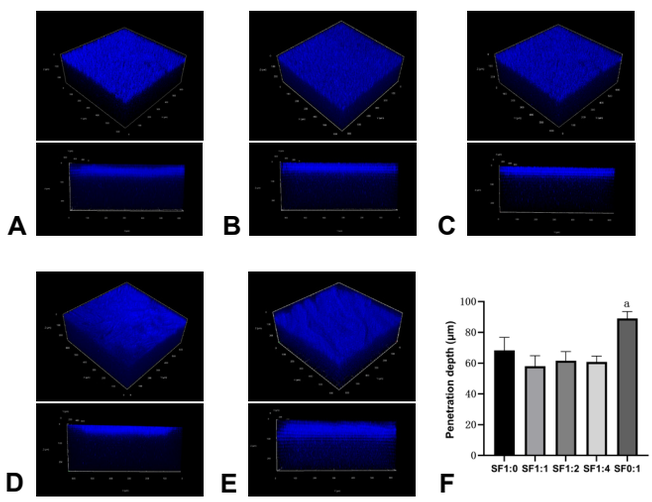

Figure 3. Top and lateral views of fibroblast nuclear fluorescence staining on SF membranes with different ratios. Group A: SF1:0; Group B: SF1:1; Group C: SF1:2; Group D: SF1:4; Group E: SF0:1. Compared with SF1:0, aP<0.05.

3.4 Guidance function for BMSCs

Calcein-AM staining results of BMSCs showed that the SF1:0 group (dense layer only) had the smallest cell penetration depth. Compared with the SF1:0 group, the penetration depths in SF1:1, SF1:2, SF1:4 and SF0:1 groups were increased, with statistically significant differences. Compared with the SF1:1 group, the penetration depths in SF1:2 and SF1:4 groups were increased. There were no statistically significant differences between SF1:2, SF1:4 groups and SF0:1 group, indicating that the porous layer of SF membranes could effectively guide BMSC penetration, and the guidance effect was optimal when the layer ratio was greater than 1:2 (Figure 4).

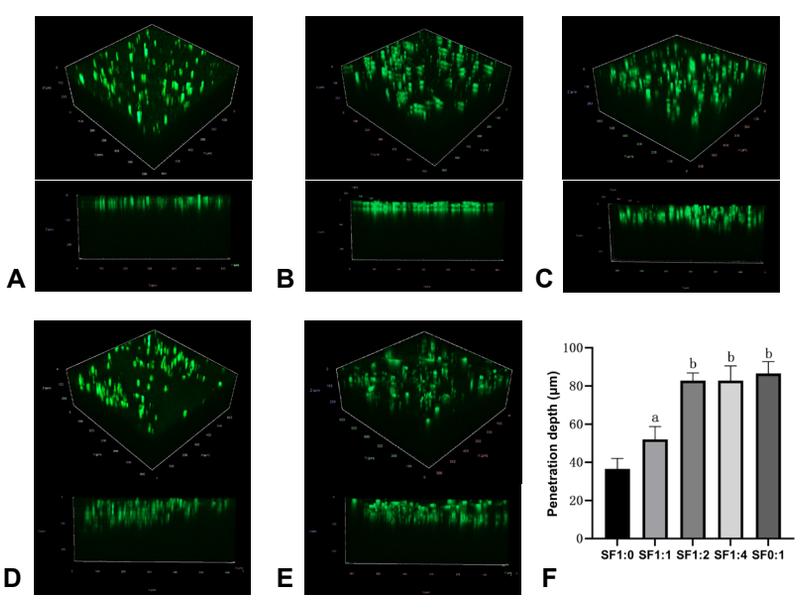

Figure 4. Top and lateral views of BMSC calcein-AM staining on SF membranes with different ratios. Group A: SF1:0; Group B: SF1:1; Group C: SF1:2; Group D: SF1:4; Group E: SF0:1. Compared with SF1:0, aP<0.05; compared with SF1:1, bP<0.05.

3.5 Establishment and treatment of rat skull defect model

Micro-CT scanning and reconstruction results showed that only a small amount of new bone was formed in the bone defect area of the blank group (no membrane implanted), with clear bone defect boundaries and no obvious bone bridge connection; the SF1:0 and SF0:1 groups had less new bone formation; the SF1:1 group had significantly more new bone formation, and part of the bone defect area was filled with new bone; the SF1:2 and SF1:4 groups had abundant new bone formation in the bone defect area, the bone defect was basically filled with new bone, the bone bridge connection was complete, and the BV/TV was significantly higher than that in other groups (Figure 5). It was shown that SF membranes promoted bone regeneration in rat skull defects, and the bone regeneration effect was optimal when the layer ratio was 1:2–1:4.

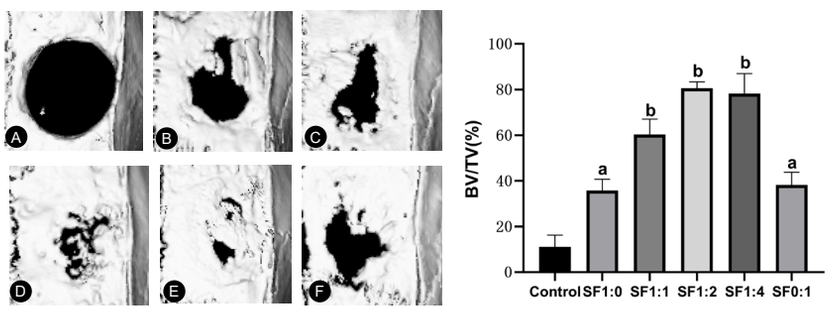

Figure 5. Micro-CT reconstruction of SF membranes with different ratios on bone regeneration in rat skull defect. Group A: blank group; Group B: SF1:0; Group C: SF1:1; Group D: SF1:2; Group E: SF1:4; Group F: SF0:1. Compared with blank group, aP<0.05; compared with SF1:0, bP<0.05.

4. Discussion

An ideal GBR membrane must simultaneously possess favorable physical barrier function, osteogenic induction activity and biocompatibility to effectively block soft tissue invasion and promote bone regeneration [12-13]. Traditional GBR membranes are difficult to meet the above dual requirements, which limits their clinical application effects. The asymmetric structure design of SF membranes provides a new idea to solve this problem. The synergistic effect of the dense layer and the loose layer is expected to achieve the dual functions of "barrier" and "induction". As a key parameter affecting the structure and function of the membrane, the optimization of the layer ratio is of great significance for the clinical application of membrane. In this study, SF membranes with different dense-to-loose layer ratios were first prepared by the particle leaching method. FTIR results showed that all membranes maintained the natural chemical structure of silk fibroin, indicating that the preparation process was stable and the change of layer ratio did not destroy the structural integrity of silk fibroin, providing a basis for its good biocompatibility and functional stability.

Excessive proliferation and invasion of fibroblasts into the bone defect area will hinder the adhesion and differentiation of osteogenic cells and inhibit bone regeneration [14-15]. In this study, it was found that the penetration depths in SF1:1, SF1:2 and SF1:4 groups were significantly lower than those in SF0:1 group, indicating that the asymmetric structure of SF membranes could effectively block fibroblast infiltration, and its dense layer played a key physical barrier role. Although the SF1:0 group (dense layer only) had certain barrier function, it could not provide growth channels for osteogenic cells due to the lack of porous layer; the SF0:1 group (loose layer only) had no dense layer, resulting in weak barrier function and easy penetration of a large number of fibroblasts, failing to block soft tissue invasion.

As the core seed cells for bone regeneration, the migration, adhesion and proliferation of BMSCs to the bone defect area are key links in bone regeneration [16-18]. This study showed that the BMSC penetration depths in SF1:2 and SF1:4 groups were significantly higher than those in SF1:0 and SF1:1 groups, with no significant difference from the SF0:1 group, indicating that the porous layer of SF membranes could effectively guide BMSC penetration, and the guidance effect was better when the layer ratio was greater than 1:2. The SF1:0 group (dense layer only) had no porous structure, making it difficult for BMSCs to penetrate and reach the bone defect area to exert osteogenic effects; the porous layer of SF1:1 group was thin, which limited the penetration and proliferation of BMSCs to a certain extent. In contrast, the SF1:2 and SF1:4 groups had suitable porous layer thickness and uniform pore structure, which could simulate the biomimetic microenvironment of natural bone tissue, providing a stable channel for the adhesion, proliferation and penetration of BMSCs, promoting the migration of BMSCs to the bone defect area and accelerating bone regeneration.

Animal experiments further verified the bone regeneration effects of SF membranes with different ratios. The BV/TV in SF1:2 and SF1:4 groups was significantly higher than those in other groups, with no significant difference between the two groups, indicating that when the layer ratio was 1:2–1:4, the membrane could simultaneously achieve favorable barrier

function and guidance ability, and effectively promote bone regeneration in rat skull defects. The low BV/TV in SF1:0 and SF0:1 group was consistent with the cell experiment results, further indicating that membrane with a single structure could not meet the dual requirements of GBR.

In conclusion, when the ratio of dense layer to loose layer of the SF membrane is designed between 1:2 and 1:4, it can simultaneously possess favorable barrier function against fibroblasts and guidance ability for BMSCs, and effectively promote bone regeneration, which is an ideal membrane ratio range in clinical GBR technology.

Acknowledgments

This study is financially supported by the Songjiang District Science and Technology Research Project of Shanghai (2024SJKJGG085).

References

[1] Buser D, Urban I, Monje A, et al. Guided bone regeneration in implant dentistry: Basic principle, progress over 35 years, and recent research activities[J]. Periodontol 2000, 2023, 93(1):25-29.
[2] Mizraji G, Davidzohn A, Gursoy M, et al. Membrane barriers for guided bone regeneration: An overview of available biomaterials[J]. Periodontol 2000, 2023, 93(1):56-76.
[3] Zhou ZL, Yun JH, Li J, et al. Comparison of the efficacy of different biodegradable membranes in guided bone/tissue regeneration: a systematic review and network meta-analysis[J]. Biomed Mater, 2023, 18(3):032003.
[4] Brum IS, Elias CN, de Carvalho JJ, et al. Properties of a bovine collagen type I membrane for guided bone regeneration applications[J]. e-Polym, 2021, 21(1):210-221.
[5] Carbonell JM, Martin IS, Santos A, et al. High-density polytetrafluoroethylene membranes in guided bone and tissue regeneration procedures: a literature review[J]. Int J Oral Surg, 2014, 43(1):75-84.
[6] Abdo VL, Suarez LJ, de Paula LG, et al. Underestimated microbial infection of resorbable membranes on guided regeneration[J]. Colloids Surf B Biointerfaces, 2023, 226:113318.
[7] Fuchs A, Youssef A, Seher A, et al. Medical-grade polycaprolactone scaffolds made by melt electrospinning writing for oral bone regeneration-a pilot study in vitro[J]. BMC Oral Health, 2019, 19:1-11.
[8] Shuai Y, Yang T, Zheng M, et al. Oriented Cortical-Bone-Like Silk Protein Lamellae Effectively Repair Large Segmental Bone Defects in Pigs[J]. Adv Mater, 2025, 37(10):e2414543.
[9] Chen W, Liu K, Liao X, et al. Harmonizing Thickness and Permeability in Bone Tissue Engineering: A Novel Silk Fibroin Membrane Inspired by Spider Silk Dynamics[J]. Adv Mater, 2024, 36(13):e2310697.
[10] Aprile P, Letourneur D, Simon-Yarza T. Membranes for Guided Bone Regeneration: A Road from Bench to Bedside[J]. Adv Healthc Mater, 2020, 9(19):2000707.
[11] Lei M, Wan HR, Song J, et al. Programmable Electro-Assembly of Collagen: Constructing Porous Janus Films with Customized Dual Signals for Immunomodulation and Tissue Regeneration in Periodontitis Treatment[J]. Adv Sci, 2024, 11(13):2305756.
[12] Lu Y, Lian XJ, Cao Y, et al. An enhanced tri-layer bionic periosteum with gradient structure loaded by mineralized collagen for guided bone regeneration and in-situ repair[J]. Int J Biol Macromol, 2024, 277:134148.
[13] Wang LJ, Wan L, Wu JX, et al. Developing a multifunctional gradient pore structure Janus membrane loaded with MB@ZIF-8 nanoparticles and hydroxyapatite for guided periodontal bone regeneration[J]. Mater Des, 2024, 244:113126.
[14] García SLA, Parada-Sanchez MT, Toro DA. The phenotype of gingival fibroblasts and their potential use in advanced therapies[J]. Eur J Cell Biol, 2020, 99(7):151123.
[15] Talbott HE, Mascharak S, Griffin M, et al. Wound healing, fibroblast heterogeneity, and fibrosis[J]. Cell Stem Cell, 2022, 29(8):1161-1180.
[16] Cui C, Zhao Y, Yan J, et al. Peptide platform for 3D-printed Ti implants with synergistic antibacterial and osteogenic functions to enhance osseointegration[J]. Mater Today Bio, 2025, 30:101430.
[17] Cheng Y, Li X, Gu P, et al. Hierarchical Scaffold with Directional Microchannels Promotes Cell Ingrowth for Bone Regeneration[J]. Adv Healthc Mater, 2024, 13(12):2303600.
[18] Xie J, Shen H, Yuan G, et al. The effects of alignment and diameter of electrospun fibers on the cellular behaviors and osteogenesis of BMSCs[J]. Mater Sci Eng C Mater Biol Appl, 2021, 120:111787.

Author Bio

Huilu Zhan (1999-), Female, Han nationality, Chinese, master candidate, Resident Physician, research direction: guided bone regeneration.